ASME 2012 5th Annual Dynamic Systems and Control Conference joint with the JSME 2012 11th Motion and Vibration Conference
DSCC2012-MOVIC2012
October 17-19, 2012, Fort Lauderdale, Florida, USA

DSCC2012-MOVIC2012-8699

ANALYSIS OF PONTRYAGIN'S MINIMUM PRINCIPLE-BASED ENERGY MANAGEMENT STRATEGY FOR PHEV APPLICATIONS

Oruganti P. Sharma*
Department of Electrical and Computer Engineering
The Ohio State University
Email: sharma.264@osu.edu

Simona Onori
Yann Guezennec#
Center for Automotive Research
#Department of Mechanical and Aeronautical Engineering
The Ohio State University
Email: onori.1@osu.edu, guezennec.1@osu.edu

ABSTRACT

This paper presents a detailed analysis of the optimal energy management problem for a plug-in hybrid electric vehicle (PHEV) solved using the Pontryagin's minimum principle (PMP). The aim of this analysis is to study the relationships between the control parameters and the vehicle and driving characteristics. In this study, a relationship between the state and co-state trajectories with the battery characteristics has been developed which has not been explored in a similar fashion in prior literature. Results from sensitivity analysis show a strong asymmetry in higher and lower estimation of the initial value of the co-state. A spatial domain analysis is also carried out which shows quasi linearity of the optimal state of charge (SOC) with respect to trip length for a combination of driving cycles. Knowledge gained from this exercise enables us to develop an adaptive energy management strategy.

INTRODUCTION

Hybrid Electric Vehicles (HEVs) and Plug-in Hybrid Electric Vehicles (PHEVs) have been recognized as a promising solution to reduce exhaust emissions and fuel consumption in the transport sector. In addition to the internal combustion engine (ICE), HEVs and PHEVs have an electric machine (EM) to provide tractive energy. Electric energy for the EM comes from the on-board battery. PHEVs differ from the HEVs as they have a larger battery pack which can be recharged from an external power source. HEV battery packs are smaller and are recharged through regeneration onboard. The presence of two power sources leads to development of an Energy Management Strategy (EMS) where both the energy sources need to be intelligently used during a driving event to minimize the operating costs of the vehicle and emissions. This paper focuses on the energy management problem in a PHEV. Unlike conventional HEV, which sustains battery State of Charge (SOC) ("charge-sustaining (CS)") over a driving event, the PHEV has the ability to deplete charge to its lowest allowable value ("charge-depleting (CD)") before it is recharged through the electricity grid. It is desirable to use as much energy from the battery as possible in a driving event. A traditional approach to tackling the PHEV-EMS problem has been by the Charge Depleting-Charge Sustaining (CD-CS) strategy which is implemented in the Chevrolet Volt. This method involves driving the PHEV in all-electric mode (CD mode) until a low SOC bound is achieved then the SOC is sustained (CS mode) until the end of the driving event. Another approach is a 'Blended' strategy where both the EM and ICE are used together throughout the driving event, intelligently depleting the battery SOC to reach its minimum bound at the end of the driving event. Prior literature shows that the blended strategy achieves better fuel economy compared to the CD-CS approach [1–3]. It enables efficient battery sizing [2]. As discussed in [4], in CD-CS mode, the battery experiences higher discharge currents. The blended strategy has lower battery C-rates and Ah-throughput (almost 30%) than that in CD-CS mode. The disadvantage of the blended mode is that the optimal cost can be achieved only when the driving event characteristics are known sl a-priori. The CD-CS strategy on the other hand, does not require prior knowledge of the driving event. This disadvantage can be addressed using Intelligent Transporation Systems (ITS), on-board Global Positioning Systems (GPSs), and Geographical Information Systems (GISs) that can provide critical information about the driving event which can be used for development

*Address all correspondence to this author.

of an optimal control strategy based on the blended mode of operation [1] [5]. It is clear that a blended strategy which takes minimal information of the driving event and provides near optimal results is desirable. A study of the optimal SOC trajectory under various driving conditions would provide valuable insight of its behavior and can be used to develop rules for a near optimal blended strategy. It is known that the global optimal solution to the energy management problem can be obtained through dynamic programming (DP) [6–8]. However it is a non-causal approach. It requires a simulator that runs backwards i.e from the end of the driving event to the beginning. Moreover, it has high time and space complexity. An alternative numerical method is the Pontryagin's Minimum Principle (PMP) [9, 10]. The PMP reduces the global optimization problem to a local minimization problem of a function called the Hamiltonian. The PMP solution has the advantage of being able to be run on a forward simulator. It is also less numerically intensive than the DP. The PMP provides a set of numerical necessary conditions for a solution to be an extremal of the problem. It has been shown for an HEV that both the DP and PMP solutions are equivalent [6]. It is also shown that these conditions become sufficient in special cases and give the global optimal solution for both HEV and PHEVs [11]. PMP has been applied in prior literature to both HEV and PHEV energy management problems [8, 12–14]. Compared to prior literature, this work provides a more detailed analysis on the selection of the initial value of the lagrangian parameter λ (λ_0). An exclusive relationship has been established between the SOC, λ trajectories and the battery characteristics. Sensitivity analysis of the fuel consumption to the parameter λ_0 shows asymmetry when the parameter is estimated higher or lower than the optimal value. Apart from time domain analysis, an analysis of the optimal SOC trajectory in the distance domain has been studied and presented in this work. The paper is divided into 5 sections. In the next section, we present the vehicle model used in this study. Then, details of the development of the PMP based EMS for the PHEV are provided. A detailed analysis of the simulation results is done. Conclusions and further work are discussed in the last section.

MODELING OF THE PHEV SIMULATOR

The simulator used in this study is modeled based off of the simulator developed at the Center of Automotive Research at the Ohio State University. It was primarily aimed at modeling a Chevrolet Equinox HEV vehicle for Challenge X student competition [6, 12, 15–17]. The initial simulator was an experimentally validated one. It has undergone modifications and improvements for the purpose of this research. It is a forward simulator which models a parallel through the road vehicle. The architecture is shown in Fig. 1, where the front axle is powered by the ICE and the rear axle by the EM[1]. The component properties are given in Tab. 1. A driver model based on PID control enforces the vehicle

[1]From a control standpoint, any vehicle architecture can be considered. The through the road hybrid architecture is under experimentation as a PHEV at Argonne National Laboratories [18] and in production by Peugeot [19] as an HEV.

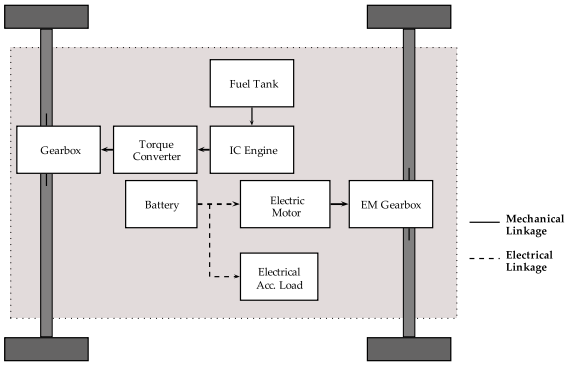

Figure 1: PARALLEL THROUGH THE ROAD ARCHITECTURE.

Table 1: COMPONENT SIZING

Component	Details
Battery	Li-ion, 17kWh / 57.5Ah (10.24 kWh usable), Cylindrical cells,cell radius 0.014m & length 0.065m 90 cells in series and 25 cells in parallel
Electric Motor	Peak 43kW@1500RPM and 274Nm@1500RPM
IC Engine	L4, 2.4Liter, Gasoline, 92.4kW@6500RPM, 176.5Nm@5000RPM
All-Electric Range	40 miles (64.3 km) (FUDS cycle)
Vehicle	1750 Kg, 2.86m wheelbase

to follow a given drive cycle by providing appropriate acceleration and braking requests. These requests are used to calculate the required torque at the wheels. The vehicle supervisory controller decides on the optimal split between the ICE and the EM to deliver the required amount of torque and also minimizes the criterion.

Powertrain and Vehicle Dynamics Modeling

A brief description of the powertrain modeling approach and the vehicle model is given in this section. A more detailed modeling section can be found in [6, 15]. A quasi-static modeling approach is adopted to model the powertrain components. The ICE model is a static model which neglects crank angle dynamics and torque oscillations. It is implemented using a torque-speed map and a fuel consumption map. The torque-speed map provides physical torque limitations of the engine at different angular velocities. The fuel consumption map is a function of engine torque and speed. The electric machine is modeled as a static model where the motor efficiency is a function of motor torque and speed. The motor torque is bounded by its physical limitations similar to the ICE. A torque converter model is implemented with a multiplication mode and lock-up mode. The multiplication mode is based of the Kotwicki model [20] and a simple lock-up logic is used. The engine torque is transmitted to the wheels through a six speed automatic gearbox. The electric machine torque is transmitted through gearbox with constant gear ratio. Both the gearboxes account for losses through a constant efficiency. The vehicle dynamics model takes into account aerodynamic drag, road grade and rolling resistance of the wheels

and give vehicle velocity resulting from the torque produced at the wheels.

Battery Model A validated [21,22] zero order equivalent circuit model is used to model the energy storage system. It is characterized by V_{oc}, the open circuit voltage, R_0, the battery internal resistance. V_L is load voltage across the cell terminals. The circuit output equation is given by:

$$V_L = V_{oc}(SOC) - I_{cell}R_0(SOC,\theta) \tag{1}$$

If P_{cell} is the power delivered by a cell then:

$$I_{cell} = \frac{V_{oc}(SOC) - \sqrt{V_{oc}(SOC)^2 - 4\cdot P_{cell}R_0(SOC,\theta)}}{2R_0(SOC,\theta)} \tag{2}$$

We consider the open circuit voltage V_{oc} as a function of SOC and the internal resistance R_0 as a function of SOC and temperature(θ). The battery temperature is a free independent parameter. It is not involved in the control formulation and is used to update the battery parameters. Equation (2) shows the non-linear nature of the battery dynamics that exists due to the dependence of the battery parameters on the SOC and θ. In the rest of the paper due to cumbersome notation, the dependence of these parameters is implied and the explicit notation is dropped. The SOC dynamics equation for the battery is given by:

$$\dot{SOC} = -\frac{I_{cell}}{Q_{cell}(\theta)} \tag{3}$$

where, Q_{cell} (amp-second) is the nominal charge capacity of the cell and is a function of temperature. The cells considered have 2.3Ah capacity and 3.3V nominal voltage. There are 90 cells in series and 25 such modules in parallel which cast together to give a total of 17Kwh (10.24 KWh usable) capacity at 297 volts. The internal resistance while charging and discharging and the open circuit voltage and have been calibrated against experimental data from Li-ion iron phosphate battery. The resistance ($R_0(SOC,\theta)$) is taken as a function of SOC and battery temperature. The open circuit voltage ($V_{oc}(SOC)$) is a function of SOC [21,22].

OPTIMAL CONTROL PROBLEM FORMULATION

The objective of the EMS is to minimize the total fuel costs in a driving event while fulfilling the torque demanded on the road by the driver. This can be formulated as a constrained optimization problem, where the mass of fuel consumed, m_f, is to be minimized over a given driving cycle, subject to dynamic and static constraints, i.e.

$$\min_u \mathcal{J} = \int_0^{t_f} \dot{m}_f(t,u)\,dt \tag{4}$$

$$s.t.\ \ \dot{SOC} = -\frac{I_{cell}}{Q_{cell}} \tag{5}$$

$$SOC_{min} \leqslant SOC \leqslant SOC_{max} \tag{6}$$

$$P_{batt_{min}} \leqslant u(t) \leqslant P_{batt_{max}} \tag{7}$$

u is the control input which is the power delivered by the battery (P_{batt}), SOC_{min} and SOC_{max} are the minimum and maximum allowable state of charge, t represents time and t_f is the total duration of the driving event. The physical limitations on the components are incorporated:

$$\begin{aligned} T_{em_{min}}(\omega_{em}) &\leqslant T_{em} \leqslant T_{em_{max}}(\omega_{em}) \\ T_{ice_{min}}(\omega_{ice}) &\leqslant T_{ice} \leqslant T_{ice_{max}}(\omega_{ice}) \end{aligned} \tag{8}$$

Here, $T_{em_{min}}$ and $T_{em_{max}}$ are the minimum and maximum possible torque values at a given angular velocity for the electric machine. Similarly, $T_{ice_{min}}$ and $T_{ice_{max}}$ are the limits of torque at a given ICE angular velocity for the ICE. The SOC dynamics equation is in the form:

$$\dot{x} = f(x,u,t) \tag{9}$$

where $x = SOC$ and $u = P_{batt}$. Unlike a conventional hybrid, for PHEV operation, it is required that the SOC go from a maximum level to minimum on completion of a driving event as given in Eq. (6). In this case, the minimum state of charge is taken as 30% and the maximum as 90%. The PMP [9] provides with a set of necessary conditions for the optimal control trajectory $u^*(t)$. The Hamiltonian function is given by:

$$\mathcal{H} = \dot{m}_f(t) + \lambda(t)\dot{x}(t) \tag{10}$$

Here, $\lambda(t)$ is the co-state which varies with time. The necessary conditions that must be satisfied by the optimal control trajectory $u^*(t)$ are:

$$\begin{aligned} &\dot{\lambda}^*(t) = -\frac{\partial \mathcal{H}(x^*(t),u^*(t),\lambda^*(t),t)}{\partial x} \\ &\dot{x}^*(t) = \frac{\partial \mathcal{H}(x^*(t),u^*(t),\lambda^*(t),t)}{\partial \lambda} \\ &x^*(0) = x(0) \\ &x^*(t_f) = SOC_{min} \\ &\mathcal{H}(x^*(t),u^*(t),\lambda^*(t),t) \leqslant \mathcal{H}(x^*(t),u(t),\lambda^*(t),t) \\ &SOC_{min} \leqslant x^*(t) \leqslant SOC_{max} \end{aligned} \tag{11}$$

The * denoting optimal policy is dropped as we consider only the optimal control policy in the remaining formulation. From Eq. (3), (10), (11):

$$\dot{\lambda}(t) = \frac{1}{Q_{cell}}\lambda(t)\cdot\frac{\partial I_{cell}(u(t),V_{oc}(x),R_0(x,\theta))}{\partial x} \tag{12}$$

λ_0 needs to be calibrated. λ_0 is tuned iteratively for each of the driving cycles considered and for varying trip lengths so that the SOC reaches the minimum SOC value at the end of the driving event. Logically, this method is non-causal as the entire driving event is to be known sl a-priori. Within the operating range of the SOC and a nominal temperature of 25^0C, the battery resistance is relatively flat and the partial derivative of R_0 with respect to x

can be assumed zero. Consider Eq. (12),

$$\dot{\lambda} = \frac{1}{Q_{cell}} \lambda \cdot \frac{\partial I_{cell}}{\partial V_{oc}} \frac{\partial V_{oc}}{\partial x} \tag{13}$$

From Eq. (2),

$$\frac{\partial I_{cell}}{\partial V_{oc}} = \frac{-I_{cell}}{\sqrt{V_{oc}^2 - 4 \cdot P_{cell} R_0}} \tag{14}$$

Consider $\frac{\dot{\lambda}}{\dot{x}}$. From Eq. (3), (13), (14),

$$\frac{\dot{\lambda}}{\dot{x}} = \frac{\lambda}{\sqrt{V_{oc}^2 - 4 \cdot P_{cell} \cdot R_0}} \cdot \frac{\partial V_{oc}}{\partial x} \tag{15}$$

From Eq. (15), it is seen that the ratio of $\dot{\lambda}$ and $\dot{x}$ is strongly related to the battery characteristics: the partial derivative of V_{oc} with x and the battery internal resistance variation with respect to SOC. Just to ensure that the final SOC does not violate the global constraint in a real time application, a penalty can be added to the cost functional. This penalty is formulated as an integral constraint as shown in [8]. The integral constraint $\phi(x(t))$ and piecewise penalty function w are given by:

$$\phi(x(t)) = w(x) \cdot \int_0^{t_f} \dot{x}(t) \tag{16}$$

$$w(x) = \begin{cases} K & \text{if } x < SOC_{min} \\ -K & \text{if } x > SOC_{max} \\ 0 & \text{else} \end{cases}$$

Here, K is a constant that is iteratively determined to ensure that the cost of using the battery is high enough or low enough to keep the SOC trajectory within the global SOC constraints. It is also possible to implement a smooth penalty function with the same behavior. $\phi(t)$ is added to the criterion function to give:

$$\mathcal{J} = \int_0^{t_f} \dot{m}_f + w(x) \cdot \dot{x}(t)\, \mathrm{d}t \tag{17}$$

The constraint appears an an additive function to the cost functional. Within the operational range of the state of charge (90% to 30%), the value of $w(x)$ is zero and does not change the original formulation.

ANALYSIS OF THE SIMULATION RESULTS

The PHEV simulator was run for different cycles with different metrics. Table 2 shows the different drive cycles along with some of their properties. FUDS is the Federal Urban Driving Schedule, FHDS is the Federal Highway Driving Schedule, MAN is a Manhattan driving cycle, US06 is a high acceleration aggressive driving schedule, WVU_{inter} is a West Virginia interstate drive cycle and WVU_{sub} is a West Virginia suburban cycle [23, 24]. The optimal SOC trajectory for repeated cycles is quasi-linear as shown in Fig. 2. It is piecewise quasi-linear for a driving event consisting of a combination of different drive cycles. If the optimum value of λ_0 is chosen, it is observed that the

Table 2: DRIVING CYCLE STATISTICS

Cycle	V_{rms} (m/s)	V_{mean} (m/s)	a_{rms} (m/s^2)	Tractive Energy per mile (MJ/km)
FUDS	11	8.8	0.63	0.29
FHDS	21.9	21.4	0.30	0.20
MAN	4.4	3.0	0.60	0.44
WVU_{inter}	17.9	15.1	0.26	0.12
WVU_{sub}	21.6	7.1	0.42	0.24
US06	24.1	21.41	0.98	0.35

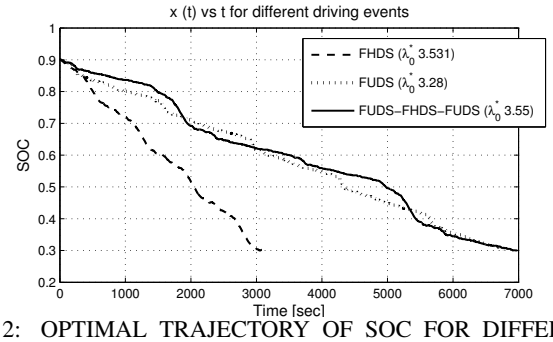

Figure 2: OPTIMAL TRAJECTORY OF SOC FOR DIFFERENT DRIVE CYCLES

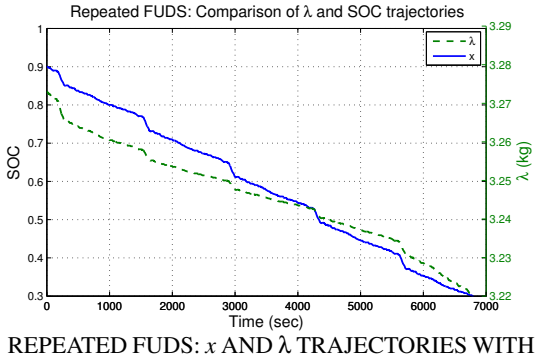

Figure 3: REPEATED FUDS: x AND λ TRAJECTORIES WITH TIME

SOC hardly ever violates the global constraints in Eq. (6). The value of λ_0 is tuned iteratively to reach SOC_{min} at the end of the driving event.

State and co-state trajectories analysis

A look at state x and co-state λ variation with time for a case of repeated FUDS cycle shows that the shapes of $\lambda(t)$ and $x(t)$ are very similar (see in Fig. 3). The ratio of $\dot{x}$ and $\dot{\lambda}$ is compared to $\frac{\partial V_{oc}}{\partial x}$ in Fig. 4 with respect to the SOC. $\frac{\dot{\lambda}}{\dot{x}}$ follows the shape of $\frac{\partial V_{oc}}{\partial x}$ over the driving cycle for FUDS. In Fig. 4, the similarity in the shape is also observed for 5 different driving events: 5 FUDS cycles, 4 FHDS cycles, 3 WVU_{inter} and a combined drive cycle consisting of a MAN cycle, WVU_{inter}, WVU_{sub}, FUDS cycle and another MAN Cycle. On the x-axis is the state of charge as it depletes during the driving event from 90% to 30%. Figure 4 confirms the result from Eq. (15), that the ratio of $\dot{\lambda}$ and $\dot{x}$ is directly related to the battery characteristics *viz.* the battery open circuit voltage variation with respect to SOC. The battery internal resistance in this case is almost flat in the operating range of the

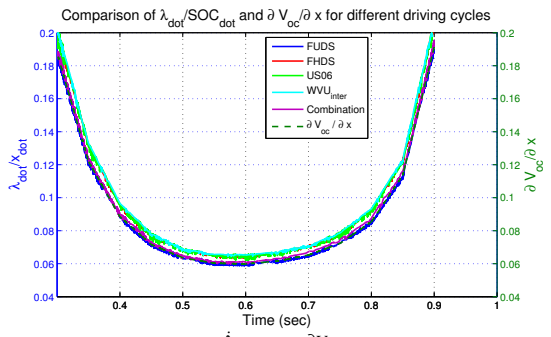

Figure 4: COMPARISON OF $\frac{\dot{\lambda}}{\dot{x}}$ AND $\frac{\partial V_{oc}}{\partial x}$ FOR DIFFERENT DRIVE CYCLES

Table 3: PERCENTAGE CHANGE IN KMPL TO CHANGE IN λ_0

	Change in λ_0^*						
Drive Cycle	-10%	-5%	-1%	1%	5%	10%	$kmpl_{conv}$
FUDS	-3.3	-2.5	-0.6	-6.3	-21.4	-36.5	-61.7
FHDS	-4.8	-3.3	-0.9	-11.7	-47.3	-59.1	-61.3
WVU	-4.9	-3.1	-0.9	-12.2	-41.5	-51.6	-59.7
$Comb_1$	-2.8	-2.1	-0.4	-7.1	-36.7	-52.0	-53.1

SOC and does not have a major effect on the ratio. The similarity in shape remains across the different drive cycles indicating independence of the shape from the drive cycle.

Sensitivity of Fuel Consumption to λ_0^*

Table 3 shows the percentage variation in kilometer per liter (kmpl), consumption for sub-optimal choices of λ_0 compared to the optimal km/l value for a trip. $Comb_1$ is a combination of manhattan and FHDS driving cycles. The table is developed for a driving event of around 80 km (50 miles). The driving distance was increased by repeating the driving cycle. Clearly, a value lower than the optimal λ_0 for a trip has a better performance than a higher estimate. For a lower estimate the penalty function is enforced when the global constraints are violated and the SOC slides along the lower boundary (30%). For a higher estimate, the split of power selected by the control strategy leads to greater use of the ICE and more fuel consumption while the battery does not discharge as much causing the km/l to be very high. $kmpl_{conv}$ is obtained from a conventional vehicle. It shows that a high estimate of λ_0 leads to km/l values comparable to the conventional vehicle. For long driving cycles (160 km), it has been seen (see Tab. 4) that a 10% higher estimate of λ_0 is less costly compared to similar estimate for 50 miles. Also, the kmpl loss becomes less sensitive to the driving cycle. Table 4 shows a 4% loss in kmpl for -10% estimate of λ_0 for the four driving cycles considered and almost 25% for a +10% estimate.

Optimal co-state variation with driving distance

The variation of the optimal λ_0 after tuning for different driving cycles is shown as a function of distance driven and RMS acceleration of the trip for different driving cycles in Fig. 5. λ_0^* is seen to be a monotonically increasing function of the distance traveled. As the distance traveled increases, the slope tends to decrease for each of the drive cycles. To determine the relationship between different drive cycles and the optimum λ_0 various metrics of the driving cycles like mean velocity, RMS-acceleration and tractive energy are considered. It is seen in Fig. 5 that the distance traveled is a stronger metric than RMS acceleration and RMS acceleration is not a sufficient metric. This was observed with other metrics as well.

Table 4: PERCENTAGE CHANGE IN KMPL TO $\pm 10\%$ λ_0 VARIATION FOR LONG DRIVING DISTANCES

Drive Cycle	-10%	10%
FUDS	-4.13	-24.82
FHDS	-3.97	-26.49
WVU	-3.92	-23.54
$Comb_1$	-4.05	-24.21

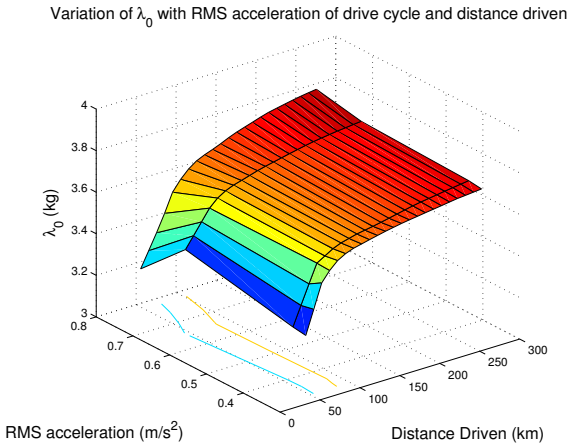

Figure 5: SURFACE PLOT OF OPTIMAL λ_0 WITH DISTANCE TRAVELED AND RMS-ACCELERATION

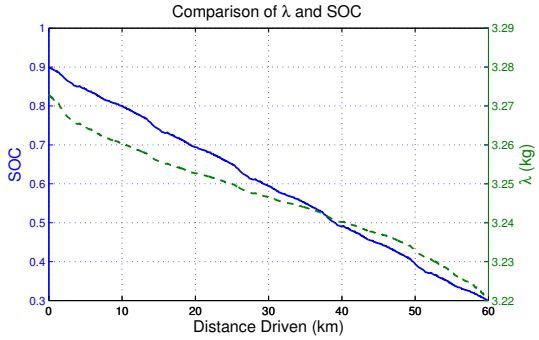

Figure 6: STATE AND CO-STATE TRAJECTORY VS DISTANCE FOR REPEATED FUDS CYCLE

Distance domain analysis

Distance to be traveled is something that can be obtained before the driving event using GPS devices. Logically, we extend the analysis from time into distance domain. The state and co-state trajectories for a repeated FUDS cycle is provided in Fig. 6. Quasi-linearity in the optimal SOC trajectory is obtained in the distance domain as well. The co-state trajectory is also shown. As observed in Fig. 4, $\dot{\lambda}^*$ is greater at the ends compared to $\dot{x}^*$ because of the nature of $\frac{\partial V_{oc}}{\partial x}$. Simulations have been done for

Table 5: LEGEND FOR DIFFERENT DRIVING CYCLES

Number	Cycle	Number	Cycle	Number	Cycle
1	FUDS	4	US06	7	Freeway
2	FHDS	5	MAN	8	Test
3	WVU_{sub}	6	WVU_{inter}	9	$Test_2$

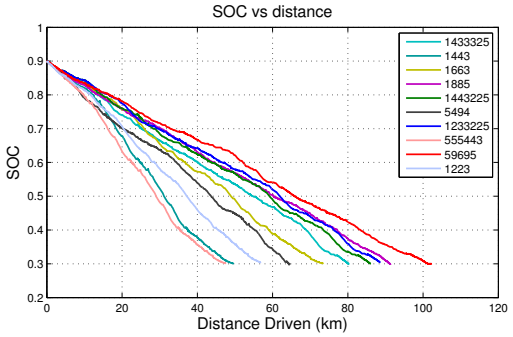

Figure 7: x^* TRAJECTORY VS DISTANCE FOR DIFFERENT COMBINATIONS OF DRIVE CYCLES

combinations of driving cycles. Each number denotes a driving cycle (see Tab. 5) and the order of the numbers gives the combination. Figure 7 shows that for the various combinations, the optimal state trajectory remains quasi-linear with respect to the distance covered. Though the state trajectory has a piecewise linear property for different driving cycles (Fig. 2) with respect to time, it remains quasi-linear in the distance domain.

CONCLUSION AND FURTHER WORK

This paper has presented an analysis of an EMS based on PMP applied to a PHEV. PMP introduces a design parameter: the Lagrangian multiplier, λ. The mathematical and simulation analysis shows that there is a strict co-relation between the battery characteristics and the trajectory of λ. The shape of $\frac{\dot{\lambda}}{SOC}$ is the same as $\frac{\partial V_{oc}}{\partial SOC}$. This is seen to be independent of the driving cycle or travel distance. The initial value of λ, λ_0, is identified as a critical calibration parameter. Various simulations were run for different travel distances and different driving scenarios and the optimal λ_0 was found iteratively. At distances around 80 km, the fuel consumption rate turns out to be very sensitive to λ_0 especially when the estimate is higher than the optimal λ_0 value. This asymmetry indicates that it is always better to have a lower estimate of λ_0 when it comes to minimizing fuel consumption. The optimum value of λ_0 is a monotonically increasing function of the distance traveled. As the distance traveled increases, the dependence of λ_0 on optimality gradually decreases. An analysis in the distance domain showed that the optimal SOC trajectory is quasi-linear for a repeated cycle and remains quasi-linear with respect to distance driven for a combination of different driving cycles. All simulations in this work were performed with zero road grade. Changes in road grade are being considered which show piecewise-linearity of optimal SOC trajectory with distance [25]. The results of this analysis will be used to develop an online practical strategy.

REFERENCES

[1] Gong, Q., Li, Y., and Peng, Z.-R., 2008. "Trip-based optimal power management of plug-in hybrid electric vehicles". *Vehicular Technology, IEEE Transactions on.,* **57**(6), pp. 3393–3401.

[2] Moura, S. J., Callaway, D. S., Fathy, H. K., and Stein, J. L., 2009. "Tradeoffs between battery energy capacity and stochastic optimal power management in plug-in hybrid electric vehicles". *Power Sources, J.,* **195**(9), pp. 2979–2988.

[3] Tulpule, P., Marano, V., and Rizzoni, G., 2009. "Effects of different PHEV control strategies on vehicle performance". In Proceedings of 2009 American Control Conference.

[4] Onori, S., Spagnol, P., Marano, V., Guezennec, Y., and Rizzoni, G., 2012. "A new life estimation method for Lithium-ion batteries in Plug-in Hybrid Electric Vehicle applications". *Power Electronics, Int. J.,* **4**(3), pp. 302–319.

[5] Zhang, C., and Vahidi, A., 2012. "Route preview in energy management of plug-in hybrid vehicles". *Control Systems Technology, IEEE Transactions on.,* **20**(2), pp. 546–553.

[6] Serrao, L., Onori, S., and Rizzoni, G., 2011. "A comparative analysis of energy management strategies for hybrid electric vehicles". *Dynamic Systems, Measurement and Control, J.,* **133**(3), p. 031092 (9 pages).

[7] Pisu, P., and Rizzoni, G., 2007. "A comparative study of supervisory control strategies for hybrid electric vehicles". *Control Systems Technology, IEEE Transactions on,* **15**(3), pp. 506–518.

[8] Sciaretta, A., and Guzzella, L., 2007. "Control of hybrid electric vehicles". *Control Systems, IEEE,* **27**(2), pp. 60–70.

[9] Kirk, D. E., 1970. *Optimal Control Theory, An Introduction*.

[10] Geering, H., 2007. *Optimal Control with Engineering Applications*. Springer.

[11] Kim, N., and Rousseau, A., 2012. "Sufficienct conditions of optimal control based on pontryagin's minimum principle for use in hybrid electric vehicles". *IMechE Part D: J. of Automobile Engineering*.

[12] Stockar, S., Marano, V., Canova, M., Rizzoni, G., and Guzzella, L., 2011. "Energy-optimal control of plug-in hybrid electric vehicles for real-world driving cycles". *Vehicular Technology, IEEE Transactions on,* **60**(7), pp. 2949–2962.

[13] Kim, N., Cha, S., and Peng, H., 2011. "Optimal control of hybrid electric vehicles based on Pontryagin's Minimum Principle". *Control Systems Technology, IEEE Transactions on.,* **19**(5), pp. 1279–1287.

[14] Serrao, L., Onori, S., Sciarretta, A., Guezennec, Y., and Rizzoni, G., 2011. "Optimal energy management of hybrid electric vehicles including battery aging". In American Control Conference.

[15] Koprubasi, K., 2008. "Modeling and control of a hybrid electric vehicle for drivability and fuel economy improvements". PhD thesis, The Ohio State University.

[16] Tulpule, P., Marano, V., and Rizzoni, G., 2010. "Energy managemernt for plug-in hybrid electric vehicles using equivalent consumption minimisation strategy". *Electric and Hybrid Vehicles, Int. J.,* **2**(4), pp. 329–350.

[17] Gu, B., 2006. "Supervisory control strategy development for a hybrid electric vehicle". Master's thesis, The Ohio State University.

[18] http://www.transportation.anl.gov/pdfs/HV/598.PDF.

[19] http://www.peugeot.com/en/products/cars/3008hybrid4.aspx.

[20] Kotwicki, A., 1982. "Dynamic Models for Torque Converter Equipped Vehicles". *SAE Technical Paper 820393*.

[21] Hu, Y., Yurkovich, S., Guezennec, Y., and Yurkovich, B., 2010. "Electro-thermal battery model identification for automotive applications". *Power Sources, J.,* **196**(1), pp. 449–457.

[22] Hu, Y., Yurkovich, S., Guezennec, Y., and Yurkovich, B., 2009. "A technique for dynamic battery model identification in automotive applications using linear parameter varying structures". *Control Engineering Practice,* **17**(10), pp. 1190–1201.

[23] http://www.epa.gov/nvfel/testing/dynamometer.htm.

[24] Wipke, K., Cuddy, M., and Burch, S., 1999. "Advisor 2.1: a user-friendly advanced powertrain simulation using a combined backward/forward approach". *Vehicular Technology, IEEE Transactions on,* **48**(6), pp. 1751–1761.

[25] Sharma, O. P., 2012. "A practical implementation of a near optimal energy management strategy based on the Pontryagin's minimum principle in a PHEV". Master's thesis, The Ohio State University.